

Fabric defect detection using linear filtering and morphological operations

H İbrahim Çelik^{1,a}, L Canan Dülger² & Mehmet Topalbekiroğlu¹

¹Textile Engineering Department, ²Mechanical Engineering Department, Gaziantep University, Gaziantep 27310, Turkey

Received 15 April 2013; revised received and accepted 16 September 2013

An algorithm with linear filters and morphological operations has been proposed for automatic fabric defect detection. The algorithm is applied off-line and real-time to denim fabric samples for five types of defects. All defect types have been detected successfully and the defective regions are labeled. The defective fabric samples are then classified by using feed forward neural network method. Both defect detection and classification application performances are evaluated statistically. Defect detection performance of real time and off-line applications are obtained as 88% and 83% respectively. The defective images are classified with an average accuracy rate of 96.3%.

Keywords: Denim fabric, Fabric defect detection, Image processing, Linear filtering, Morphological operation, Neural network

1 Introduction

The deformed regions which damage the appearance and the fabric performance include '*fabric defect*'. In modern weaving technology, many types of fabric defects are still occurring because of many reasons such as yarn quality used in the weaving, weaving preparation operations or weaving mechanics. Having completed the weaving process, the defective regions of the fabric are detected by the quality control workers. The worker scans the fabric of about 2 m wide with his/her eyes and detects the defects. He/she then records them with their types. Since quality evaluation of the fabric varies depending on the experience and concentration of the worker, this process cannot be achieved objectively. It is observed that inspection speed of a fabric even woven with an efficiency of 97% is about 30 m/min.

There is a growing need for automated fabric defect inspection system in the textile industry. The fabric inspection process may be achieved in shorter time and with higher performance by using an automatic fabric inspection system. The fabric defects can be evaluated objectively and presented statistically. The employment cost may be reduced.

Many attempts have been made to replace the traditional human inspection by automated visual systems. Image processing (IP) routines and artificial intelligence (AI) methods are used for automatic defect detection. Different types of image acquisition

devices such as digital camera, CCD line-scan camera, area scan camera and scanner are used for capturing the fabric images.

Karayiannis *et al.*¹ have presented a pilot system for defect detection and classification of web textile fabric in real-time. A method based on double thresholding, binary filtering, binary labeling, multi-resolution decomposition via wavelet transform, and statistical texture feature extraction was presented. Eight types of classification were performed, namely no error, black vertical error, white vertical error, wrinkle, black horizontal error, white horizontal error, black spot, and white spot.

Mak *et al.*² have proposed a prototype of real-time computer vision system for detecting defects in fabrics. The study also proposed a filter selection method which could automatically tune the Gabor functions to match with the texture information. The tests were performed both on-line and off-line using the prototype system. It is noted that the maximum detection speed of the prototype system was 15 m/min and 276 images were captured and analyzed. Seventeen images contained defects and the rest were all defect-free. All these defects occurred in 17 fabric images were successfully detected. The defect types studied in this work were harness breakdown, miss pick, warp burl and water damage.

Zhao *et al.*³ have performed fast fourier transform (FFT) and self-adaptive power spectrum (SAPS) decomposition. Sector-regional energy of spectrum was extracted and its mean and the standard deviation were taken as the fabric features. They were given as

^aCorresponding author.
E-mail: hcelik@gantep.edu.tr

inputs into the classifier such as BPNN. The defect type tested in this study was ‘slub’. The recognizable defect rate was more than 95% for defects of which area was more than 2 mm² and more than 80% for defects of which area was less than 2 mm².

Kumar⁴ has presented an approach for the segmentation of local textile defects using feed-forward neural network (FFN) and fast web inspection method using linear neural network. A twill weave fabric sample with defect miss pick was tested by using FFN method. Fabric inspection image with the defects slack-end, dirty-yarn, miss pick and thin bar were tested by using linear neural network method. Plain weave fabric samples with defect double weft, thin bar, broken ends and slack-pick were used for real time defect detection with FFN method.

Anagnostopoulos *et al.*⁵ were presented an algorithm based on simple statistical measurements, thresholding and morphological operations. The algorithm was tested in a total sample of 50 images for 5 types of commonly occurring defect images and for each type 10 image samples.

Stojanovicw *et al.*⁶ have presented a fabric defect inspection system. The defect detection algorithm was consisted of binary image processing, statistical texture analysis and run time code (RTC) neural classification. The proposed system showed a speed of 120m/min with a recognition rate of 86.2%.

Cho *et al.*⁷ have presented a prototype system for real-time fabric defect detection. The system was developed only for the detection of the existing defect without classifying them. The proposed system was designed to extract minimal-sized defects without classifying the kinds of defects because of the speed. The inspection algorithm was applied with an inspection speed of 250 mm /s. The defects inspected by the system were warp float, broken pick, hole and oil spot. It was stated that nearly perfect recognition rate was obtained on an oily spot and spot. However, the recognition rate of warp and pick float was about 80%. The size and position of defects were determined and saved.

In this study, an algorithm for denim fabric defect detection has been developed by using linear filtering (LF) and morphological operations. The defective fabric images are then classified by using FFNN. The algorithm is applied both real-time by using a machine vision system⁸ and off-line by using database images. Undyed denim fabric is selected as material for the study. The denim fabric samples are woven on

Picanol Gammex rapier weaving machines with production speed of 450 rpm and production efficiency of 85%. The algorithm is applied on five different defect types, namely warp lacking, weft lacking, soiled yarn, hole and knot or yarn flow. The defective areas of the fabric images are detected successfully and the boundary of the defect is labeled. Both real-time and off-line performances of the algorithm are evaluated statistically with comments. The classification accuracy of the network is also tested and evaluated statistically.

2 Materials and Methods

A fabric defect database was prepared for off-line application. The database included defect-free fabric and five commonly occurring defects, namely warp lacking, weft lacking, hole, soiled yarn and knot. Thirty different samples were prepared for each defect type and defect-free fabric. One hundred eighty (180) fabric samples were provided in total. The sizes of the fabric samples prepared were kept as 5.5 cm × 23.5 cm. The image frames of the database were acquired by means of a scanner with a resolution of 200 dpi.

A machine vision system was used for real-time application (Fig. 1). The fabric sample was placed on fabric inspection machine. A CCD camera system was placed on the fabric inspection machine with a proper illumination unit⁸. As the fabric was wound, the image frames were captured and then they were analyzed on the computer. The fabric motion and the image acquisition process were synchronized with a rotary encoder via a frame grabber card (Fig. 1).

2.1 Defect Detection Algorithm

The algorithm is developed by using linear filtering (LF) and morphological operations. Linear filters are

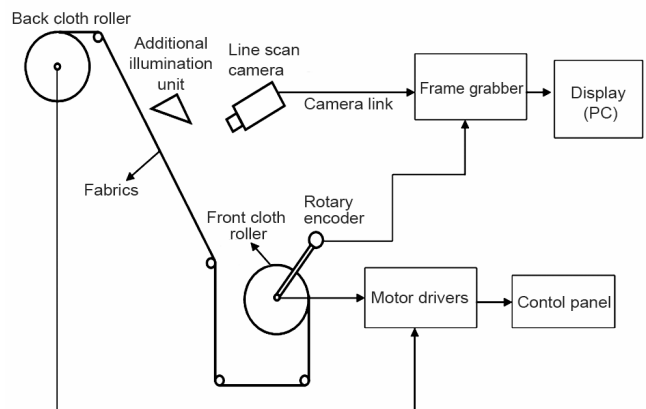


Fig. 1—Experimental set-up

used to segment the defective region. The morphological operations are used to remove the noises and to make the defective area clearer. The defective region of the fabric image is identified according to the gray level intensity of each pixel. Two thresholding values (upper and lower thresholds) are determined by using the defect-free fabric image as a template. The gray level values of the detected image are compared with these threshold values. If the pixel value is between the thresholds, it is stated as ‘defect-free’, otherwise the pixel is determined as ‘defective’.

The flowchart for LF application is given in Fig. 2. The image frames are captured from the scanner or CCD camera. Pixel values do not reflect the true intensities of the real scene. This is simply the noise resulted from errors in the image acquisition process. The noises are then seen because of illumination change, fabric structure and impurities available in the fabric. They are removed by using Wiener low-pass filter and mean filter.

Wiener estimates the local mean [Eq. (1)] and the variance [Eq. (2)] around each pixel⁹, as shown below:

$$\mu = \frac{1}{NM} \sum_{n_1, n_2 \in n} a(n_1, n_2) \quad \dots (1)$$

$$\sigma^2 = \frac{1}{NM} \sum_{n_1, n_2 \in n} a^2(n_1, n_2) - \mu^2 \quad \dots (2)$$

where n_i ($i=1,2$) is the $N \times M$ local neighborhood of each image pixel in the image ‘a’. Wiener filter makes its estimation by using following equation⁹:

$$b_{(n_1, n_2)} = \mu + \frac{\sigma^2 - v^2}{\sigma^2} [\alpha(n_1, n_2) - \mu] \quad \dots (3)$$

where v^2 is the noise variance.

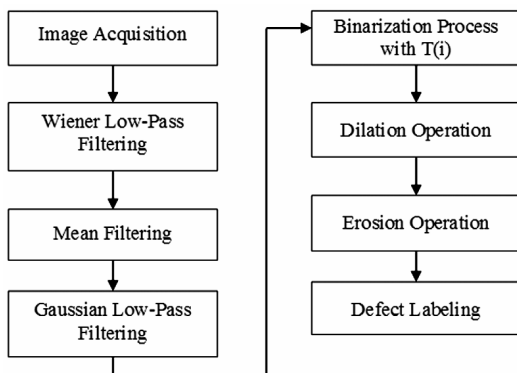


Fig. 2—Flowchart of the algorithm

The image filtered by Wiener method is applied by the mean value filter. The mean value (the low-pass filter) removes the high-frequency noise. The intensity value of each pixel in the image substitutes for the average intensity value of the surrounding pixels. The window size is necessary to determine the neighbor of a pixel, it is experimentally selected as 3×3 . Because each pixel gets set to the average of the pixels in its neighborhood, local variations caused by noises are reduced. The Gaussian filter is used for image smoothing as low-pass filter. The image frame is convolved with the Gaussian function¹⁰, as show below:

$$h_g(n_1, n_2) = e^{-\frac{(n_1^2 + n_2^2)}{2\sigma^2}} \quad \dots (4)$$

where, n_1 and n_2 are the locations of the related pixel; and σ^2 , the variance of neighborhood.

The filtered image is converted into the binary form. Thus, the defective area is identified and clarified. The binarization process is achieved by using the double thresholding method. This method finds the maximum and minimum threshold values on each pixel of the axis direction during inspection. These values are calculated by using the average and the standard deviation values of a defect-free image frame^{6,9}, as shown below:

$$T_{1,2} = \text{mean} [\alpha(i, j)] \pm w * \text{mean} [\text{std}(\alpha(i, j))] \quad \dots (5)$$

where T_1 is the upper limit; T_2 , the lower limit of the double thresholding processes; and w , the weighting factor, experimentally between 2-4. The upper and lower thresholding limits are determined by using a defect-free fabric image as a template. The binarization process is carried out^{7,2,11} using the following equation.

$$L(i, j) = \begin{cases} 0, & T_1 < \alpha(i, j) < T_2 \\ 1, & \alpha(i, j) < T_1 \text{ or } \alpha(i, j) > T_2 \end{cases} \quad \dots (6)$$

If the pixel value of the detected image is between T_1 and T_2 , the gray value is allocated as 0. Otherwise, it is set as 1 because of the high defect probability. In the binary image, the value of 0 means no defect, and 1 means that the cell has a defect or noise.

The binary image is applied to dilation operation and the spaces between the defective regions are

closed but they are interconnected. Then the remaining noises are removed via erosion operation. The dilation and erosion operations are indicated as $A \oplus B$ and $A \ominus B$ respectively; where B is the structuring element and it slides over the image A from the top to the left bottom right by applying convolution with the same area of the image. The dilation operation means that the center pixel of the structuring element is placed on each background pixel. If any of the neighborhood pixels is foreground pixels with value 1, then the background pixel is changed to foreground. In the erosion operation, the centre pixel of the structuring element is placed on each foreground pixel with value 1. If any of the neighborhood pixels is background pixels with value 0, then the foreground pixel is switched to background^{12,13}. Finally, the defective area is labeled.

2.2 Feature Extraction

The defective fabric images are automatically classified according to their texture features by using FFNN method. The texture features are assessed as the network input values and the defect classification is obtained as the output. A feature extraction algorithm is performed by using discrete wavelet transform (DWT), soft wavelet thresholding (SWT)¹⁴ and gray level co-occurrence matrix (GLCM) methods¹⁵. The feature vector includes the first order and second order statistical properties. The first order statistical properties¹⁶ consist of *average gray level*, *average contrast*, *smoothness*, *third moment*, *uniformity* and *entropy*. They are derived from the intensity histogram of the gray level image. The second order statistical properties¹⁷⁻¹⁹ include *energy*, *contrast*, *correlation*, *variance*, *inverse difference moment*, *sum average*, *sum variance*, *sum entropy*, *entropy*, *difference variance*, *difference entropy* and *information measure of correlation 1 and 2*. The second order statistics are derived from GLCM of images by using the methodology proposed by Haralic¹⁷. The feature vector is extracted by applying the following steps:

- (i) The noises of the image are removed by means of Wiener filter. A smoother image is obtained.
- (ii) The filtered image is applied DWT at level 2 by using 'db3' wavelet base and the image is decomposed into sub-images. The approximation image is applied to SWT¹⁴.
- (iii) The image is then applied with 'Laplacian' operator. Regular defect-free texture of the

fabric is made smoother and the defective area is accentuated.

- (iv) The 1st order statistics are then extracted from the convolved image¹⁶.
- (v) The weave pattern is composed by interlacing the warp and weft yarns and by arranging them in horizontal and vertical directions in fabric. The co-occurrence matrices with offset [0, 1] are formed for horizontal and vertical detail coefficients of decomposed sub-images. They represent the latitude and longitude properties of the fabric.
- (vi) The 2nd order statistics are finally extracted from the co-occurrence matrices by using Haralick method¹⁷⁻¹⁹.
- (vii) The feature column vector of the defective image is formed by using the first and second order statistics. The vector has got 32 elements.

The procedure given above is repeated for each defective fabric image.

2.3 Neural Network Architecture

In this study, four defect types, namely hole, warp lacking, weft lacking and soiled yarn, are classified by using FFNN method. A two layer network is formed by using MATLAB[®]. The hidden layer has got 37 neurons and the output layer has got 4 neurons. The feature vectors of 25 images are extracted for each defect type. The input matrix with the size of 32×100 is obtained. The network is trained by using this input matrix. Scaled conjugate gradient back propagation method is used for training. The mean square error (MSE) algorithm adjusts the biases and weights so as to minimize the mean square error. MSE of training, testing and validation operations are calculated as 0.0021, 0.00014 and 0.00027 respectively.

3 Results and Discussion

The defective areas of the fabric sample are detected successfully and the boundaries of them are labeled in Figs 3 and 4. In order to judge the sensitivity of the algorithm, the warp lacking [Fig. 3(a)] has got a width of 1 mm and the weft lacking [Fig. 3(c)] has got 2 mm.

The method is applied on 180 database images for off-line application and 606 images for real-time application. The performance evaluations are achieved according to statistical criteria such as; true detection (TD), false detection (FD), misdetection (MD) and overall detection (OD). OD is the sum of TD and FD. Various application performances are discussed hereunder:

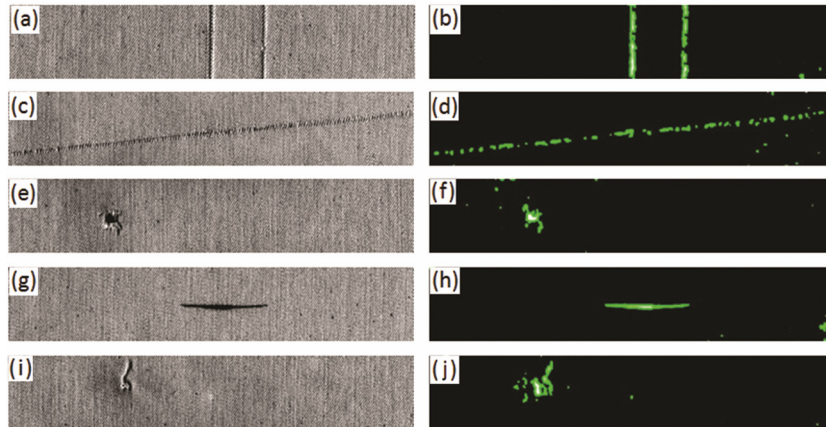


Fig. 3—Off-line detection of warp lacking (a), weft lacking (c), hole (e), soiled yarn (g) and knot (i). The respective defect segmentation results are shown in (b), (d), (f), (h) and (j)

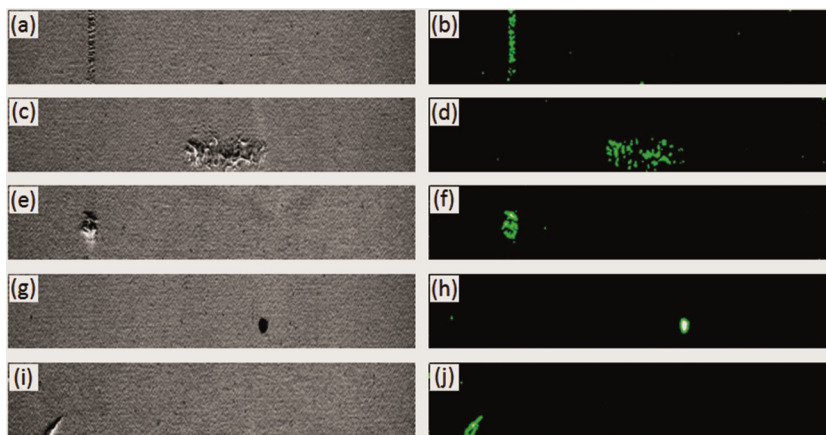


Fig. 4—Real-time detection of warp lacking (a), weft lacking (c), hole (e), soiled yarn (g) and knot (i). The respective defect segmentation results are shown in (b), (d), (f), (h) and (j)

(i) Off-line Application Performance

Off-line defect detection performance of the method is presented in Table 1. All defect types and defect-free samples are detected with TD over 83%. The lowest TD rate is obtained for weft lacking and knot defects. The highest TD is obtained for warp lacking. Any MD does not occur for all database images (Table 1). TD rates of hole and soiled yarn defect types are found to be the same. Similarly, the knot and weft lacking defects have the same TD rates.

(ii) Real-time Application Performance

Real-time defect detection performance of the method is presented in Table 2. TD rates are over 88%. The lowest TD rate is obtained for warp lacking defect with 88.5%. OD rates are over 96% (Table 2).

MD is only detected for yarn flow. Among five defect types the highest TD rates are obtained for hole and soiled yarn.

(iii) Classification Application Performance

Having trained the neural network successfully, 20 samples of each type of defects are used to test for the network classification accuracy. The overall accuracy rate of each defect type is presented in Table 3. The defective images are classified with an average accuracy rate of 96.3%. As the hole defect is recognized with 100% accuracy rate, the others are recognized with a rate of 95%. Since many weft yarns are removed and the large spaces occur between the yarns, one of the weft lacking images is recognized as the hole. One of the soiled yarn images is recognized as warp lacking because of having large vertical soil.

Table 1—Off-line application performance evaluation

Parameter	Image frame type					
	Defect-free	Warp lacking	Weft lacking	Hole	Soiled yarn	Knot
Total number of frames	30	30	30	30	30	30
TD	27	28	25	26	26	25
FD	3	2	5	4	4	5
MD	0	0	0	0	0	0
OD	30	30	30	30	30	30
TD rate, %	90.0	93.3	83.3	86.7	86.7	83.3
FD rate, %	10.0	6.7	16.7	13.3	13.3	16.7
MD rate, %	0.0	0.0	0.0	0.0	0.0	0.0
OD rate, %	100.0	100.0	100.0	100.0	100.0	100.0

Table 2—Real-time application performance evaluation

Parameter	Image frame type					
	Defect-free	Warp lacking	Weft lacking	Hole	Soiled yarn	Yarn flow
Total number of frames	227	104	57	86	78	55
TD	225	92	55	85	77	50
FD	2	12	2	1	1	3
MD	0	0	0	0	0	2
OD	227	104	57	86	78	53
TD rate, %	99.1	88.5	96.5	98.8	98.7	90.9
FD rate, %	0.9	11.5	3.5	1.2	1.3	5.5
MD rate, %	0.0	0.0	0.0	0.0	0.0	3.6
OD rate, %	100.0	100.0	100.0	100.0	100.0	96.4

Table 3—Defect classification accuracy rates

Defect type	Hole	Warp lacking	Weft lacking	Soiled yarn	Number of sample	Classification accuracy, %
Hole	20	0	0	0	20	100
Warp lacking	0	19	1	0	20	95
Weft lacking	1	0	19	0	20	95
Soiled yarn	0	1	0	19	20	95

4 Conclusion

All defect types and defect-free samples are detected with TD rate over 83% for off-line application and with TD rate over 88% for real-time application. Four defect types, namely hole, warp lacking, weft lacking and soiled yarn are classified by using FFNN method. The defective images are classified with an average accuracy rate of 96.3%.

Acknowledgement

Authors wish to thank Gaziantep University Scientific Research Projects Management Unit for funding project ‘Development an Intelligent System for Fabric Defect Detection’ (project code-MF.10.12).

References

- 1 Karayiannis Y A, Stojanovic R & Mitropoulos P, *Defect detection and classification on web textile fabric using multiresolution decomposition and neural networks*, paper presented at the 6th IEEE International Conference on Electronics, Circuits and Systems, Pafos, 1999.
- 2 Mak K L, Peng P & Lau H Y K, *A real-time computer vision system for detecting defects in textile fabrics*, paper presented at the IEEE International Conference on Industrial Technology, China, 2005.
- 3 Zhao D X, Wang H, Zhu J L & Li J L, *Research on a new fabric defect identification method*, paper presented at IEEE International Conference on Computer Science and Software Engineering, 2008.

- 4 Kumar A, *Pattern Recog*, 36 (2003) 1645.
- 5 Anagnostopoulos C, Vergados D, Kayafas E, Loumos V & Stassinopoulos G, *Visualization Computer Animation*, 12 (2001) 31.
- 6 Stojanovic R, Mitropulos P, Koulamas C, Karayiannis Y, Koubias S & Papadopoulos G, *Real-Time Imaging*, 7 (2001) 507.
- 7 Cho C S, Chung B M & Moo-Jin P, *IEEE Transac Industrial Electronics*, 52 (2005) 1073.
- 8 Çelik H İ, *Development of an intelligent fabric defect inspection system*, PhD thesis, Gaziantep University, 2013.
- 9 <http://www.mathworks.com/help/toolbox/images/ref/wiener2.html>. (accessed on 06.12.2012)
- 10 <http://www.mathworks.com/help/toolbox/images/ref/fspecial.html#bqkft1d>. (accessed on 06.12.2012)
- 11 Mak K L & Peng P, *World Acad Sci, Eng Technol*, 13 (2006) 75.
- 12 Kim S, Bael H, Cheon S P & Kim K B, *Comput Sci its Applications– ICCSA*, 3483 (2005) 1075.
- 13 Serdaroglu A, Ertuzun A & Ercil A, *Pattern Recog Image Analy*, 16(1) (2005) 61.
- 14 *Wavelet Toolbox for use with Matlab* (The MathWorks, Inc.), 1997.
- 15 *Image Processing Toolbox™ 6 User’s Guide* (The MathWorks, Inc.), 2009.
- 16 Gonzalez R C, Woods R E & Eddins S L, *Digital Image Processing using Matlab* (Prentice-Hall Inc., New Jersey), 2004, 666-669.
- 17 Haralick R M, *Proceedings of the IEEE*, 67 (5) (1979) 786.
- 18 Alam F I & Uddin Faruqui R U, *Eur Sci Res*, 50(4) (2011) 543.
- 19 Haralick R M, Shanmugam K & Dinstein I, *IEEE Transactions on Systems, Man and Cybernetics*, 3(6) (1973) 610.